

Magnetic resonance spectroscopy outperforms perfusion in distinguishing between pseudoprogression and disease progression in patients with glioblastoma

Mohamed E. El-Abtah[†], Pratik Talati[†], Melanie Fu, Benjamin Chun, Patrick Clark, Anna Peters, Anthony Ranasinghe, Julian He, Otto Rapalino, Tracy T. Batchelor, R. Gilberto Gonzalez, William T. Curry, Jorg Dietrich, Elizabeth R. Gerstner, and Eva-Maria Ratai

Athinoula A. Martinos Center for Biomedical Imaging, Charlestown, Massachusetts, USA (M.E.E., P.T., M.F., B.C., P.C., A.P., A.R., J.H., R.G.G., E.M.R.); Department of Neurosurgery, Massachusetts General Hospital, Boston, Massachusetts, USA (P.T., W.T.C.); Department of Radiology, Massachusetts General Hospital, Boston, Massachusetts, USA (O.R., R.G.G., E.M.R.); Harvard Medical School, Boston, Massachusetts, USA (O.R., T.T.B., R.G.G., W.T.C., J.D., E.R.G., E.M.R.); Brigham and Women's Hospital, Neurosciences Center, Boston, Massachusetts, USA (T.T.B.); Massachusetts General Hospital Cancer Center, Boston, Massachusetts, USA (W.T.C., J.D., E.R.G.)

[†]These authors contributed equally.

Corresponding Author: Eva-Maria Ratai, PhD, Athinoula A. Martinos Center for Biomedical Imaging, Department of Radiology, Massachusetts General Hospital, 13th Street, Building 149, Room 2301, Charlestown, Massachusetts, USA (eratai@mg.harvard.edu).

Abstract

Background. There is a need to establish biomarkers that distinguish between pseudoprogression (PsP) and true tumor progression in patients with glioblastoma (GBM) treated with chemoradiation.

Methods. We analyzed magnetic resonance spectroscopic imaging (MRSI) and dynamic susceptibility contrast (DSC) MR perfusion data in patients with GBM with PsP or disease progression after chemoradiation. MRSI metabolites of interest included intratumoral choline (Cho), myo-inositol (ml), glutamate + glutamine (Glx), lactate (Lac), and creatine on the contralateral hemisphere (c-Cr). Student *T*-tests and area under the ROC curve analyses were used to detect group differences in metabolic ratios and their ability to predict clinical status, respectively.

Results. 28 subjects (63 ± 9 years, 19 men) were evaluated. Subjects with true progression ($n = 20$) had decreased enhancing region ml/c-Cr ($P = .011$), a marker for more aggressive tumors, compared to those with PsP, which predicted tumor progression (AUC: 0.84 [0.76, 0.92]). Those with true progression had elevated Lac/Glx ($P = .0009$), a proxy of the Warburg effect, compared to those with PsP which predicted tumor progression (AUC: 0.84 [0.75, 0.92]). Cho/c-Cr did not distinguish between PsP and true tumor progression. Despite rCBV (AUC: 0.70 [0.60, 0.80]) and rCBF (AUC: 0.75 [0.65, 0.84]) being individually predictive of tumor response, they added no additional predictive value when combined with MRSI metabolic markers.

Conclusions. Incorporating enhancing lesion MRSI measures of ml/c-Cr and Lac/Glx into brain tumor imaging protocols can distinguish between PsP and true progression and inform patient management decisions.

Key Points

- Patients with true progression have elevated Lac/Glx and decreased ml/c-Cr.
- Perfusion indices marginally improved the ROC/AUC compared to the MRSI markers.

Importance of the Study

The standard of care for patients with glioblastoma (GBM) is surgical resection followed by chemoradiation. Despite improving survivorship, a common issue is determining whether new or increased contrast-enhancement on MRI post chemoradiation represents recurrent tumor or treatment effects (pseudoprogression). We report that MR spectroscopic measures of the Warburg effect (lactate/glutamine + glutamate; Lac/Glx) and myo-inositol normalized to contralateral hemisphere creatine (ml/c-Cr) can differentiate between GBM progression

and pseudoprogression. Despite relative cerebral blood volume (rCBV) and relative cerebral blood flow (rCBF) being individually predictive of tumor response, they added no additional predictive value when combined with MRSI metabolic markers. To the best of our knowledge, this is the first use of multi-echo time in vivo MR spectroscopy to report that lower ml/c-Cr and elevated Lac/Glx within the enhancing volume are predictive of true disease progression, highlighting the value of this method in brain tumor imaging protocols.

Glioblastoma (GBM) is the most aggressive type of primary central nervous system tumor, with a median survival of 15 months and a 2-year survival rate of 8–12%.^{1,2} The standard of care for patients with GBM is surgical resection of the tumor followed by concomitant radiation and chemotherapy as described in the Stupp protocol.³

Despite improving survivorship rates under the Stupp protocol, a common issue is determining whether new or increasing contrast-enhancement on a T1-weighted brain MRI are expected treatment effects—termed pseudoprogression (PsP)—or tumor. The majority of PsP cases occur within the first 3 months after completion of chemoradiotherapy, although it can occur up to 6 months or longer after treatment, which complicates the clinical decision-making process.^{4–6} Therefore, there is an unmet clinical need to distinguish between PsP and true tumor progression during the early course of treatment to aid in the decision to continue surveillance or initiate other treatment options such as anti-angiogenic therapy, targeted therapy, or immunotherapy.⁷

Due to limitations of standard MRI sequences in determining PsP from tumor progression, there has been an increased interest in incorporating advanced MR modalities. Several studies have used MR spectroscopic imaging (MRSI) to investigate the enhancing region after chemoradiation. Rabinov et al. conducted 3T MR spectroscopy on 14 subjects who had histopathologically-confirmed PsP or true progression to show that Choline (Cho), a marker of cellular proliferation and membrane turnover, normalized to normal Creatine (Cr) distinguished between radiation effects and recurrent tumor in gliomas.⁸ Another group has shown that elevated Cho, coupled with decreased *N*-acetylaspartate (NAA, a marker of neuronal integrity), was a marker of disease progression.⁹ An elevated lipid peak, associated with cellular membrane disruption and necrosis, when accompanied with decreased Cho and NAA has been suggested to reflect an inflammatory response and is predictive of PsP.¹⁰ Importantly, these studies did not incorporate multi-echo MR spectroscopy data to investigate other potential biomarkers of tumor progression which are detectable with short echo times (TE) such as myo-inositol (ml) and glutamate (Glu) + glutamine (Gln), commonly referred to as Glx.

GBM results in disruption of the blood brain barrier, which in turn causes changes in osmotic regulation. Lower levels of myo-inositol (ml) have been shown in more aggressive gliomas, and it has been recently reported that shorter-term survivors of recurrent glioblastoma treated with antiangiogenic therapy had lower intratumoral ml normalized to Cr in the contralateral normal-appearing white matter tissue (c-Cr) compared to longer-term survivors.^{11,12} In addition to serving as a central nervous system osmoregulator, ml is a marker of astrocytic gliosis and is elevated in response to brain inflammation, insult, or low-grade gliomas, highlighting its potential in distinguishing between PsP and true progression.^{13,14}

Growing tumors also undergo active metabolic reprogramming in a phenomenon called the Warburg effect.¹⁵ The metabolic shift from oxidative phosphorylation to anaerobic glycolysis shunts glucose towards lactate (Lac) production and decreased glutamate (Glx) generation. Recently, deuterium MR spectroscopy imaging showed metabolic differences in Lac/Glx, a proxy for the Warburg effect, in a rat glioma model and two human subjects, although to our knowledge, this marker has yet to be applied to investigate the tumor environment during treatment with chemoradiation.¹⁶

Perfusion imaging methods can relay information regarding tumor vascular permeability and blood volume, both of which tend to be elevated in disease progression, making it a potentially useful tool to distinguish between PsP and true progression.¹⁷ The most common method is dynamic susceptibility contrast (DSC) imaging, which has been utilized to study PsP. A retrospective study by Gahramanov et al. on 68 patients found that increased contrast-enhancement in conjunction with low relative cerebral blood volume (rCBV) was suggestive of PsP whereas higher levels of rCBV accompanied by contrast-enhancement likely suggested true progression.¹⁸ Interestingly, a recent meta-analysis reported that perfusion imaging parameters such as rCBV may not be the ideal method for differentiating PsP from glioma recurrence but may serve to increase the diagnostic accuracy in combination with other imaging modalities.¹⁹

The purpose of this study was to elucidate mechanistic differences between PsP and true progression in patients

with pathology-confirmed GBM after chemoradiation using the multi-echo MRSI metabolites Cho/c-Cr, ml/c-Cr, and Lac/Glx. Furthermore, we assessed the prognostic utility of tumor perfusion to distinguish between PsP and true progression, and whether it can provide added value when combined with MRSI markers.

Materials and Methods

Patient Recruitment

This study was approved by the institutional review board. All patients had histologically confirmed cases of GBM, underwent surgical resection, were at least 18 years old, and had a baseline Karnofsky Performance Score (KPS) \geq 50. Patients were treated based on the Stupp protocol and received concomitant chemotherapy and involved-field radiation therapy (IFRT) delivery consisting of 60 Gy over 30 fractions to the tumor region. Chemotherapy treatment plans included temozolomide (75 mg/m² daily during radiation therapy, followed by 150–200 mg/m² on 5 consecutive days of each 28-day cycle for up to 6 months following completion of radiation therapy).

All patients were discussed by a multidisciplinary team. Patients were classified as clinical PsP based on a new enhancing or enlarging enhancing mass on MR imaging that was then stable on subsequent imaging as read by a clinical neuro-radiologist or a biopsy of the enhancing region showing no evidence of malignant cells and only treatment changes as read by a clinical neuropathologist in the context of a stable clinical course. Three out of the eight subjects (37.5%) who were classified as PsP in our study had histopathological confirmation of treatment effect. On the other hand, patients with clinical disease progression had progressive radiographic changes on MR imaging or a biopsy confirming recurrent disease and/or progressive clinical decline (in KPS score or increased steroid use).

Magnetic Resonance Imaging

MR data was acquired with either 3.0T Siemens scanners (MAGNETOM Prisma and MAGNETOM Skyra, Siemens Healthineers, Erlangen, Germany) or 1.5T GE scanners (Signa HDx and HDxt, GE Medical Systems, Milwaukee, WI, USA). Standard MRI parameters for pre- and post-contrast T1-weighted images are described elsewhere.²⁰

Patients underwent 3D MRSI on the Siemens scanners. MRSI data was obtained via localization by adiabatic selective refocusing (LASER) using spiral k-space readout as described in Andronesi et al.²¹ Acquisition parameters included echo time (TE) = 30 and 135 ms, TR = 1700 ms, resolution = 1 cm³, acquisition time = 2 \times 7 min, acquisition matrix = 160 \times 160 \times 80 mm, field of view (FOV) = 160 \times 160 \times 80 mm and slab thickness = 40 mm. Water suppression was achieved through a technique called water suppression enhanced through T1 effects (WET).²²

Patients underwent 2D MRSI on the GE scanners. MRSI data was obtained using product point-resolved spectroscopy (PRESS) with phase encoding. Acquisition

parameters included TE = 30 ms and 135 ms, TR = 1500 ms, resolution = 1.44 cm³, acquisition time = 2 \times 8 min, acquisition matrix = 180 \times 180 mm, slice thickness = 10 mm, and FOV = 220 mm. Water suppression was achieved via Chemical Shift Selective methods (CHESS).²³ Across both MRSI sequences, short and intermediate TE data was obtained since short TE is useful for detecting the Glx and ml peaks, whereas intermediate TE can help distinguish between the lactate and lipid signal.^{24,25}

Notably, the MRSI data was obtained after acquisition of the T1-weighted post-contrast MRI scans and was overlaid on T1-weighted post-contrast images for spectral classification. We could not estimate the absolute metabolites using unsuppressed water signal as reference because acquiring an extra dataset of unsuppressed water would substantially increase scan time, which was not feasible within a clinical context. Voxels of interest (VOI) were classified as enhancing disease if $>50\%$ of the voxel was enhancing as depicted in Figure 1. Subsequently, the average metabolic ratios within the enhancing region were calculated as previously described.²⁶

LCModel 6.3 Software was used to process the raw spectra based on available basis sets of various metabolites.²⁷ Pre-processing (coil combine and frequency shift correction) of the GE data was performed with Spectroscopy Analysis by General Electric (SAGE) software (GE Healthcare). All spectra were examined by a clinical spectroscopist with over 18 years of experience. Only spectra with full width at half maximum (FWHM) of singlets <15 Hz and signal to noise ratio (SNR), defined as the highest peak divided by the standard deviation of the noise of the residual between the spectrum and the fit, ≥ 2 were included in the analyses as previously described.²⁰ We assessed the following metabolites: Cho, ml, Lac, and Glx. All metabolites were quantified as ratios over the contralateral normal-appearing white matter to avoid bias as tumoral creatine has been shown to be decreased in GBMs and other tumors.²⁸ Lastly, we calculated Lac/Glx as a proxy for the Warburg effect. We did not correct for the effect of glycine (Gly) to the ml signal at short TE, as it has been previously shown that its contribution is consistent across enhancing and contralateral voxels.¹²

For the perfusion analysis, patients were administered 0.1 mmol/kg of a gadolinium-based contrast agent (Magnevist® or Dotarem® through an IV) as part of a DSC imaging protocol using the following parameters: TR = 1500 ms, TE = 40/30 ms (GE/Siemens), FOV = 220 \times 220 mm², matrix = 128 \times 128, slice thickness = 5 mm, and slice gap = 1 mm. Enhancing lesions were manually segmented on the T1-weighted post-contrast image using 3D Slicer²⁹ and imported into nordicICE (NordicNeuroLab, Norway) to generate leakage-corrected relative cerebral blood flow (rCBF) and relative cerebral blood volume (rCBV) maps as described by others.^{29,30} Of note, macrovascular contribution was removed from the perfusion maps via thresholding of the top 5% of voxels.

Statistical Analysis

Receiver operating characteristic (ROC) curves, area under the ROC curves for metabolite ratios and perfusion

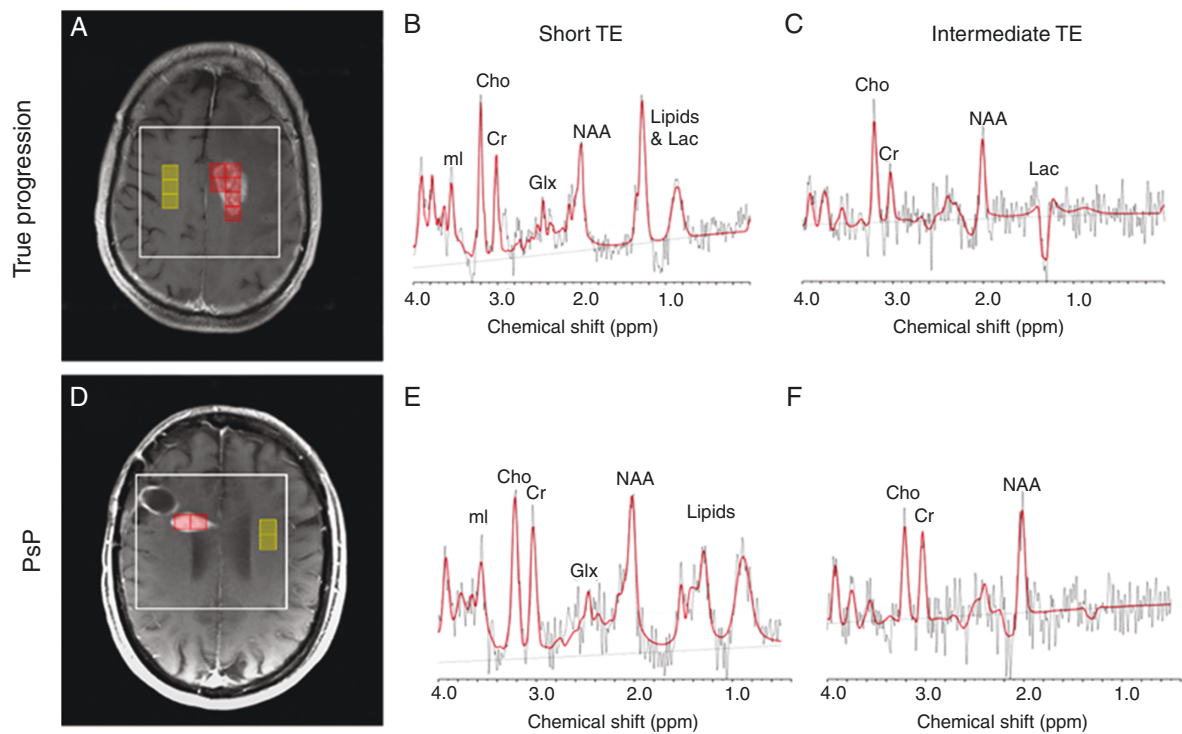


Figure 1. Representative MRS voxel selection for two subjects at different echo times. Left panel represents axial T1-weighted post-contrast images in the radiological orientation for a subject with true progression (A) and PsP (D). The box surrounding the representative voxels and enhancing lesion represents the MRS volume of interest, the boxes overlaid on the enhancing lesion represent the voxels from which the average Cho, Lac, Glx, and ml metabolite ratios were averaged, and the boxes overlaid on the contralateral hemisphere represent the voxels which were used to quantify the contralateral creatine which served as denominator for average Cho/c-Cr, ml/c-Cr, Lac/c-Cr, and Glx/c-Cr. The middle panel illustrates short echo time (TE) spectra obtained from a single voxel within the enhancing region for a patient with disease progression (B) and PsP (E). The right panel illustrates intermediate TE spectra obtained from a single voxel within the enhancing region for a patient with disease progression (C) and PsP (F). Lac, lactate; NAA, *N*-acetylaspartate; Cho, choline; Cr, creatine; ml, myo-Inositol; Glx, glutamate/glutamine.

markers, Student *T*-tests, Likelihood Ratio Test, Wilcoxon Rank Sum Exact Test, and Spearman rank correlation coefficient were calculated using JMP Pro 15 (SAS, Singapore). A marker was considered effective when the lower bound of the 95% Wald confidence interval (CI) was >0.5 . All continuous demographic data (eg, age, KPS score, time to MR data acquisition) underwent Mood's Median Test for group differences while categorical variables underwent Chi-square test. Due to the hypothesis-generating nature of our analyses, no correction for multiple comparisons was performed. A *P* value $< .05$ was considered significant unless otherwise specified.

Results

Demographics

There were 28 subjects, with 8 classified as PsP and 20 as true tumor progression at the time of scan acquisition (Table 1). There were no group differences regarding age ($P = .10$), median time in days from completion of radiation therapy to MR data acquisition ($P = .41$), gender ($P = .14$), race ($P = .24$), IDH1 status ($P = .42$), and MGMT

status ($P = .58$). Patients with PsP had significantly higher KPS score than those with true progression (Table 1). Representative spectra for a patient with PsP and disease progression are shown in Figure 1 at two different echo times. One subject was included in both groups (ie, true progression and PsP) due to longitudinal spectroscopy data when that subject was determined to have initial PsP and then subsequent true progression (Figure 2).

Inter-scanner and Magnetic Field Strength Variability

Firstly, we assessed whether interscanner variability was a significant covariate for distinguishing between PsP and true progression as four patients were scanned on GE scanners and 24 patients were scanned on Siemens scanners. Based on Likelihood Ratio tests, scanner type was an insignificant predictor of clinical status compared to enhancing volume Cho/c-Cr ($P = .55$), ml/c-Cr ($P = .22$), Lac/Glx ($P = .64$), rCBV ($P = .35$), and rCBF ($P = .43$). Furthermore, based on Wilcoxon Rank Sum Tests, there were no significant differences in average enhancing volume Cho/c-Cr ($P = .87$), ml/c-Cr ($P = .38$), Lac/Glx ($P = .68$), rCBV ($P = .46$), and rCBF ($P = .56$) between GE and Siemens scanners.

Table 1. Patient demographics

Demographics	PsP	Progression	Total	P-value
Age in years, median \pm SD (range)	58 \pm 12.11 (27–66)	64 \pm 6.0 (53–81)	63 \pm 8.83 (27–81)	.10
Male gender (%)	7 (88%)	12 (60%)	19 (68%)	.14
Race (Black/White)	0/8	2/18	2/28	.24
Baseline KPS, median \pm SD (range)	90 \pm 8.35 (70–90)	80 \pm 11 (70–90)	80 \pm 6.39 (70–90)	.006
Median time (in days) of data acquisition \pm SD	160 \pm 1785	227 \pm 331	222 \pm 996	.41
IDH1 mutant/wildtype/unknown	0/7/1	2/18/0	2/25/1	.42
MGMT methylated/unmethylated/unknown	3/4/1	5/15/0	8/19/1	.58

There are no differences in age, gender, race, median time of MR data acquisition, IDH, and MGMT status across groups. However, there is a significant group difference for baseline median KPS between patients with disease progression and pseudoprogression (PsP).

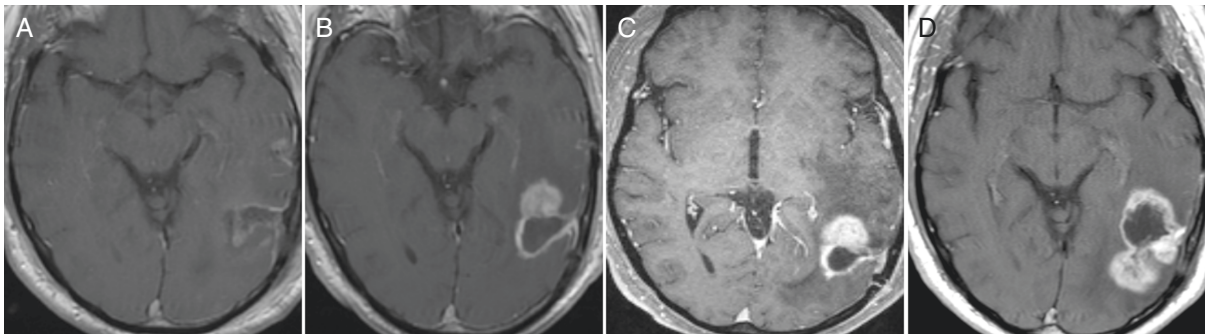


Figure 2. Longitudinal T1-post-contrast MRI demonstrating transition from PsP to true progression for a single subject. (A) Is the post-operative MRI after surgical resection of a left temporo-occipital GBM. The patient was subsequently initiated on a chemoradiation protocol, and the three-month follow-up scan demonstrated new enhancement as shown in (B). This mass was stable on the next follow-up MRI obtained a month later generating a diagnosis of PsP (C). However, there was increased enhancement three months later, accompanied by clinical decline, indicating disease progression (D).

Cho/c-Cr as a Predictor of PsP versus True Progression

Previous studies have shown that Cho/c-Cr in the enhancing volume can distinguish between recurrence and PsP.^{8,31} We also assessed the ability of Cho/c-Cr to predict PsP versus true progression. There were no differences in Cho/c-Cr between those with true progression and PsP. The former had a mean Cho/c-Cr of 0.51 whereas the latter had a mean value of 0.35, which was not statistically significant ($P = .24$). Furthermore, Cho/c-Cr was unable to distinguish between PsP and true recurrence as illustrated by an AUC of 0.56 (CI: 0.45, 0.73). A statistical summary can be in [Supplementary Table 1](#).

mI/c-Cr as a Predictor of PsP Versus True Progression

Based on previously published findings that enhancing mI/c-Cr ratios are decreased in shorter-term survivors of recurrent GBM immediately prior to and during bevacizumab-based therapy, we tested whether patients with true progression would display lower mI/c-Cr.¹² In

the enhancing region, patients with PsP had significantly higher mI/c-Cr ratios compared to patients with true progression ($P = .011$) ([Figure 3A](#)). Elevated mI/c-Cr within the enhancing VOI was predictive of PsP with an AUC of 0.84 (CI: 0.76, 0.92) ([Table 2](#)) and the associated ROC curve is shown in [Figure 3B](#). Contingency analyses in the enhancing VOI revealed that 92% of patients with mI/c-Cr lower than 0.73 had true progression.

Lac/Glx as a Predictor of PsP versus True Progression

We investigated whether a marker of the Warburg effect, Lac/Glx, could help distinguish between those with PsP versus true recurrence levels.¹⁶ Within the enhancing VOI, subjects with true progression had significantly higher Lac/Glx ratios compared to those with PsP ($P = .0009$) ([Figure 3A](#)), which was predictive of clinical status as illustrated by an AUC of 0.84 (CI: 0.75, 0.92) ([Table 2](#)). The associated ROC curve is shown in [Figure 3C](#), and subsequent contingency analyses revealed that ninety-one percent of patients with Lac/Glx greater than 0.30 within the enhancing VOI had true progression.

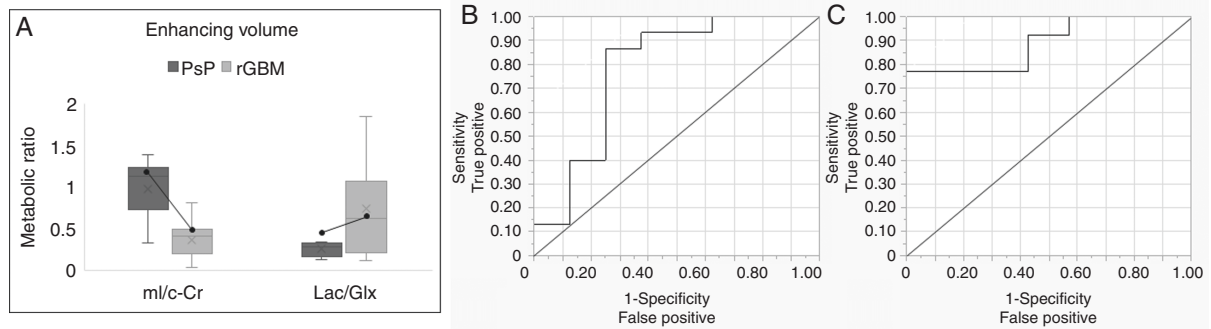


Figure 3. Metabolic levels of ml/c-Cr and Lac/Glx within the enhancing volume stratified by clinical status. (A) Box and whisker plots depict that subjects with PsP had higher mean ml/c-Cr and lower Lac/Glx in the enhancing VOI compared to those with true progression. Longitudinal changes in ml/c-Cr and Lac/Glx from PsP to true progression in a single subject are depicted by a black dot connected by a solid line. ml/c-Cr decreased by 56% and Lac/Glx increased by 114% when transitioning from PsP to true progression. The ROC curve for both markers, ml/c-Cr (B), and Lac/Glx (C) is illustrated.

Table 2. Statistical summary of metabolic biomarkers

Marker	Enhancing VOI AUC (CI)
ml/c-Cr	0.84 (0.76, 0.92)
Lac/Glx	0.84 (0.75, 0.92)
rCBV	0.70 (0.60, 0.80)
rCBF	0.75 (0.65, 0.84)

AUC and 95% confidence intervals (CI) for tumor status prediction are included for the enhancing volume of interest (VOI). Significant AUCs (lower bound of the 95% CI greater than 0.50) are bolded.

We performed exploratory analyses to determine whether the aforementioned results were driven by Lac or Glx. Therefore, we individually assessed Lac/c-Cr and Glx/c-Cr and found that both were predictive of clinical status. Specifically, patients with PsP had lower mean ratios of enhancing Lac/c-Cr compared to those with true progression (0.61 vs. 1.09; $P = .032$) which was predictive of clinical status with an AUC of 0.75 (CI: 0.65, 0.84). On the other hand, those with PsP had elevated mean Glx/c-Cr compared to those with true recurrence (2.08 vs. 1.05; $P = .031$) which was predictive of clinical status with an AUC of 0.74 (CI: 0.65, 0.84). A statistical summary of these two additional metabolic predictors is highlighted in [Supplementary Table 1](#).

Longitudinal Changes in ml/c-Cr and Lac/Glx in Transitioning from PsP to True Progression

Since there was one subject in our study who had longitudinal MRSI data starting from when they were determined to have PsP and eventually exhibited true progression, we investigated whether this patient would exhibit similar metabolic changes in ml/c-Cr and Lac/Glx. At the time of PsP, the average enhancing volume ml/c-Cr and Lac/

Glx ratios were 1.13 and 0.29, respectively. However, after transitioning to true progression, the enhancing volume ml/c-Cr decreased by 56% and the Lac/Glx increased by 114% ([Figure 3A](#)).

DSC Imaging as a Predictor of PsP Versus True Progression

Sample rCBV and rCBF maps are shown for a subject with PsP and true progression ([Supplementary Figure 1](#)). Patients with true progression had a trend towards increased rCBV compared to patients with PsP ($P = .08$) but had significantly elevated rCBF ($P = .04$) ([Figure 4A](#)). Elevated rCBV (AUC: 0.70; CI: 0.60, 0.80) and rCBF (AUC: 0.75; CI: 0.65, 0.84) were both predictive of true progression ([Table 2](#)), and the associated ROC curves are illustrated in [Figure 4B](#) and [C](#).

Multimodal DSC and Spectroscopic Analyses

We investigated whether a combination of the enhancing VOI metabolic markers and DSC-derived perfusion measures would result in increased predictive value as measured by AUC. Combining intratumoral MRSI measures of ml/c-Cr, Lac/Glx with rCBV generated an AUC of 0.81, which did not outperform ml/c-Cr or Lac/Glx. The combination of ml/c-Cr, Lac/Glx, and rCBF only lead to a marginal increase in the AUC to 0.85.

Finally, we explored whether there was a correlation between the perfusion markers and the metabolic ratios using Spearman rank correlation coefficient. There was a strong negative correlation between enhancing VOI ml/c-Cr and rCBF ($\rho = -0.50$; $P = .05$). Although there was also a negative correlation between enhancing volume ml/c-Cr and rCBV, this did not reach the threshold for significance ($\rho = -0.21$; $P = .44$). The metabolic measure for the Warburg effect, Lac/Glx, did not statistically correlate with perfusion metrics.

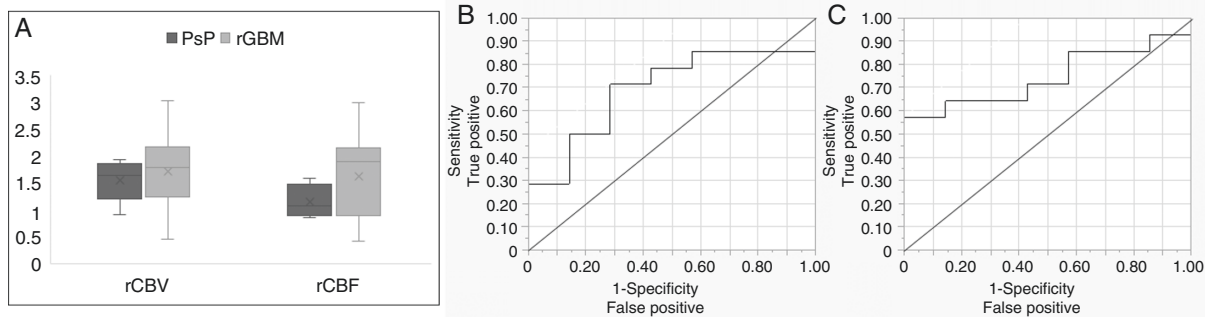


Figure 4. rCBV and rCBF stratified by clinical status. (A) Box and whisker plots depict that subjects with true progression had significantly higher mean rCBF ($P = .04$) but not rCBV ($P = .08$). The ROC curve for both markers, rCBV (B) and rCBF (C) is illustrated.

Discussion

Conventional imaging methods have difficulty discerning increased contrast-enhancement during treatment as disease progression or PsP. In this study, we used multi-echo MRSI using short and intermediate TE and found that two emerging biomarkers, ml/c-Cr and Lac/Glx, can distinguish between PsP and disease progression. The DSC data provided mixed results about distinguishing between PsP versus true progression; while rCBF was significantly different between the groups, rCBV was not able to distinguish between pseudoprogression and true progression. Furthermore, it did not enhance the ability of the MRSI markers to predict tumor status, as measured by AUC.

GBMs are characterized by a highly hypoxic environment, which facilitates tumor invasion as well as resistance to radiotherapy and chemotherapy.³² The association between anaerobic metabolism, hypoxia, and lactate, as detected by MRSI, was highlighted in a recent animal model.¹⁶ Aggressive tumors shift towards anaerobic metabolism, resulting in elevated levels of Lac and decreased levels of Glx. In line with these mechanisms, patients with true disease progression in our dataset displayed significantly elevated Lac/Glx ratios within the enhancing VOI compared to those with PsP, suggesting a mechanistic switch that occurs in the critical months after chemoradiation. This is further illustrated in the longitudinal case study, where the subject had a 114% increase in Lac/Glx between PsP and true progression, suggesting a transformation of the enhancing region with time to a more aggressive phenotype. This highlights the potential sensitivity of MRSI to capture these metabolic changes for a single subject, and to that end, a need to track longitudinal changes in metabolic markers in patients with GBM.

Our finding that ml/c-Cr can distinguish between PsP and true progression, highlights the utility of this short echo time metabolite. Lower ml levels have been reported in more aggressive gliomas and in patients failing anti-angiogenic therapy.^{11,12} One possible mechanism is that ml contributes to phosphatidylinositol (PI), which when phosphorylated leads to downstream signaling mechanisms

that ultimately activate metalloprotease-2 (MP-2), which, as suggested Castillo et al., can lead to tumor spread.¹¹ As MP-2 is generated, less ml is available, resulting in lower levels in more aggressive tumors. Another possible explanation is that this finding can be driven by blood brain barrier (BBB) and micro-vasculature breakdown in patients with recurring disease. The presence of actively proliferative and infiltrative tumors results in substantive damage to blood vessels which subsequently results in less osmoregulation and subsequently less ml.

While MRSI has been used in other studies to distinguish PsP from true progression,^{33,34} these studies were limited in metabolite assessments acquired during a single echo time. For example, in one of the first studies published on this topic using MRSI, Rabinov et al. showed that choline normalized by contralateral creatine can distinguish between radiation effects and recurrent tumor.⁸ However, there are notable differences between that study and the present one. First, of the 14 patients in the study, only 4 had GBM which is a limited sample size to consolidate the robustness of their proposed marker in distinguishing between PsP and true progression in this population. Second, Cho is a marker that is known to be elevated not only in tumor proliferation, but also cellular destruction from radiation effects and inflammatory signals.^{35,36} This can further complicate the clinical assessment of PsP versus true progression as the metabolic ratio will be elevated in both cases, regardless of enhancement status. This may partly explain our finding that Cho/c-Cr was a poor metabolic marker in distinguishing between those with PsP and true tumor progression. On the other hand, we show that myo-inositol, glutamate + glutamine, and lactate are different between patients with PsP and true progression after chemoradiation which may reflect the underlying tumor physiology, and not just membrane turnover. Finally, Rabinov and colleagues only used intermediate echo time spectroscopy to detect Cr, NAA, lipids, and Lac, limiting their ability to resolve short echo time metabolites that were critical in our dataset for distinguishing PsP from true progression.⁸ As our study suggests, there is substantial clinical utility in acquiring short echo time metabolites such as Glx and ml.

Although our finding that DSC imaging in isolation is also predictive of outcome, the combination of rCBV and rCBF with the metabolic markers resulted in negligible increases to the AUC. This finding suggests that the metabolic markers alone are sufficient to predict PsP versus true progression and supports the recent meta-analysis that perfusion imaging alone may not be sufficient in differentiating PsP from glioma recurrence.¹⁹ Furthermore, the differential group finding between rCBV and rCBF could be due to the small sample size or tumor uncoupling of perfusion values. This study is valuable within a clinical setting as clinicians can potentially incorporate MRSI into clinical scans to distinguishing between PsP and true progression without adding sequences of low diagnostic utility.

Several other groups have used different modalities to distinguish PsP from tumor progression such as PET imaging and machine learning algorithms. Several groups in Europe have used amino acid tracers such as ¹¹C-methionine (MET), ¹⁸F-fluoroethyl-L-tyrosine (FET), and L-3,4-dihydroxy-6-¹⁸F-fluorophenylalanine (F-DOPA), for the metabolic imaging of brain tumors.^{37–39} Despite being predictive of survivorship, PET imaging may not be able to distinguish between PsP and true progression, even at 10 weeks follow-up.⁴⁰ Even though there is increasing emphasis on using machine learning algorithms to distinguish between PsP and true progression based on lesion shape, margin, texture, and eccentricity, its use within the clinical setting is limited due to its extensive post-processing and inability to account for confounding artifacts.^{41,42}

The novelty of our research lies in the incorporation of multi-echo MRSI data to elucidate a mechanism that may explain the metabolic differences observed in the enhancing volume of those with PsP and true disease progression. Notably, ml is an understudied marker, that has been previously implicated as a prognosticator of survivorship in those with recurrent GBM treated with antiangiogenic agents,^{12,14} but never as a marker to distinguish between PsP and disease progression. Although we were limited by a small sample size, the results of this retrospective study suggest that decreased levels of ml/c-Cr are a robust marker of disease progression as opposed to treatment effects, and therefore, a prognosticator of poor outcome. Furthermore, using multi-echo MR spectroscopy, we were able to show that Lac/Glx, a proxy for the Warburg effect, resulted in an excellent classifier to predict true progression vs. treatment induced changes.

We acknowledge that there are some limitations in our study. First, our sample size was small but serves as a foundational study for which other groups can build upon with larger data sets. Second, histopathological assessment has been regarded as the gold standard for distinguishing between tumor progression and treatment effect.⁵ However, the majority (62.5%) of the patients with PsP in our cohort were made by a radiological assessment and clinical follow-up assessment with consideration of steroid use by the interdisciplinary team as per the response assessment in neuro-oncology (RANO) criteria.⁴³ This is a clinically accepted method of distinguishing between treatment effects and true progression after chemoradiation, especially since performing biopsies carries a non-negligible risk, is an invasive examination, and requires suitable conditions.⁴⁴ Given that the decisions

regarding disease progression or pseudoprogression in our cohort were made taking many different clinical and radiographic factors into account, the possibility of a systematic error remains low. It is worth highlighting that biopsies are also susceptible to sampling bias and suffer from a lack of standardized methodology which can limit clinician's ability to make an accurate diagnosis of PsP versus true progression in cases of histologically "mixed" patterns.⁴⁵ Third, the MRSI data from our cohort was derived from different vendors and magnetic field strengths. However, we showed that scanner effect was not a confounder, and previous reports have showed that greater magnetic field strength simply improves SNR without substantially impacting metabolite ratios.^{46,47} Our incorporation of 1.5T and 3T scanners may enhance the generalizability of our study as our results show that regardless of field strength, ml/c-Cr and Lac/Glx can be quantified to reveal robust differences between those with PsP and true progression. Finally, it should be noted that obtaining MRSI data does require technical expertise both in data acquisition and processing, which limits its widespread integration.²⁰

Conclusion

In conclusion, our results suggest that ml/c-Cr, a surrogate for tumor aggressiveness, and Lac/Glx, a proxy marker for the Warburg effect, can distinguish between PsP and true progression. DSC imaging adds little to no additional predictive value when compared with MRSI metabolic markers alone. There may be utility in incorporating MRSI with clinical scans to help distinguish between PsP and true progression.

Supplementary Material

Supplementary material is available at *Neuro-Oncology Advances* online.

Supplementary Figure 1. Sample rCBV and rCBF maps. rCBV and rCBF maps are shown for a subject with PsP (A) and true progression (B).

Keywords

glioblastoma (GBM) | lactate (Lac) | magnetic resonance spectroscopic imaging (MRSI) | myo-inositol (ml) | pseudoprogression (PsP).

Funding

This study was supported by the National Institutes of Health (R01CA190901 and R01DA047088 to E.M.R., 2P50CA165962, U19 CA264504, 5K12CA090354, and 5P30CA006516 to T.T.B.) and a National Cancer Institute Proton Beam Federal Share Grant to W.T.C. and E.R.G.

Acknowledgments

We thank all participating Massachusetts General Hospital neuro-oncologists, Cancer Center and Radiology staff, and Quantitative Tumor Imaging staff for assisting in this study.

Conflict of Interest Statement. M.E.E. No relevant relationships P.T. No relevant relationships M.F. No relevant relationships B.C. No relevant relationships P.C. No relevant relationships A.R. No relevant relationships J.H. No relevant relationships O.R. Support from GE Healthcare for travel expenses as a presenter T.T.B. National Institutes of Health (NIH) grant to institution; royalties from Wolters Kluwer as an author for UpToDate; consulting fees from ONO Pharmaceuticals; NIH committee co-chair; leadership roles with the American Academy of Neurology and Society for Neuro-Oncology R.G.G. No relevant relationships W.C. IMRIS, Deerfield Imaging (Board of Directors) J.D. Royalties from Wolters Kluwer as an author for UpToDate; consulting fees from Blue Earth Diagnostics and Unum Therapeutics. E.R.G. No relevant relationships E.M.R. BrainSpec Inc (Scientific Advisory Board).

Authorship Statement. Experimental design: M.E.E., P.T., T.T.B., W.C., O.R., R.G.G., J.D., E.R.G., and E.M.R. Implementation: M.E.E., P.T., M.F., B.C., P.C., A.P., A.R., J.H., O.R., R.G.G., W.C., J.D., E.R.G., and E.M.R. Data analysis/interpretation: M.E.E., P.T., M.F., B.C., P.C., A.P., A.R., J.H., O.R., R.G.G., W.C., J.D., E.R.G., and E.M.R. Manuscript drafts/revisions: M.E.E., P.T., T.T.B., and E.M.R. Approved final manuscript: all authors.

References

- Hanif F, Muzaffar K, Perveen K, Malhi SM, Simjee SU. Glioblastoma multiforme: a review of its epidemiology and pathogenesis through clinical presentation and treatment. *Asian Pac J Cancer Prev*. 2017; 18(1):3–9.
- Ghosh M, Shubham S, Mandal K, et al. Survival and prognostic factors for glioblastoma multiforme: retrospective single-institutional study. *Indian J Cancer*. 2017; 54(1):362–367.
- Stupp R, Mason WP, van den Bent MJ, et al. Radiotherapy plus concomitant and adjuvant temozolomide for glioblastoma. *N Engl J Med*. 2005; 352(10):987–996.
- Lee J, Wang N, Turk S, et al. Discriminating pseudoprogression and true progression in diffuse infiltrating glioma using multi-parametric MRI data through deep learning. *Sci Rep*. 2020; 10(1):20331. <https://www.nature.com/articles/s41598-020-77389-0>
- Clarke JL, Chang S. Pseudoprogression and pseudoresponse: challenges in brain tumor imaging. *Curr Neurol Neurosci Rep*. 2009; 9(3):241–246.
- Winter SF, Vaios EJ, Muzikansky A, et al. Defining treatment-related adverse effects in patients with glioma: distinctive features of pseudoprogression and treatment-induced necrosis. *Oncologist*. 2020; 25(8):e1221–e1232.
- Chen W, Liu D, Liu P, et al. Current evidence and challenges of systematic therapies for adult recurrent glioblastoma: results from clinical trials. *Chin J Cancer Res*. 2021; 33(3):417–432.
- Rabinov JD, Lee PL, Barker FG, et al. In vivo 3-T MR spectroscopy in the distinction of recurrent glioma versus radiation effects: initial experience. *Radiology*. 2002; 225(3):871–879.
- Sawhani V, Taylor R, Rowley K, et al. Magnetic resonance spectroscopy for differentiating pseudo-progression from true progression in GBM on concurrent chemoradiotherapy. *Neuroradiol J*. 2012; 25(5):575–586.
- Aquino D, Gioppo A, Finocchiaro G, Bruzzone MG, Cuccarini V. MRI in glioma immunotherapy: evidence, pitfalls, and perspectives. *J Immunol Res*. 2017; 2017:5813951. <https://www.hindawi.com/journals/jir/2017/5813951/>
- Castillo M, Smith JK, Kwok L. Correlation of myo-inositol levels and grading of cerebral astrocytomas. *Am J Neuroradiol*. 2000; 21(9):1645–1649.
- El-Abtah ME, Wenke MR, Talati P, et al. Myo-inositol levels measured with mr spectroscopy can help predict failure of antiangiogenic treatment in recurrent glioblastoma. *Radiology*. 2022; 302(2):410–418.
- Zahr NM, Mayer D, Rohlfing T, Sullivan EV, Pfefferbaum A. Imaging neuroinflammation? A perspective from MR spectroscopy. *Brain Pathol*. 2014; 24(6):654–664.
- Steidl E, Pilatus U, Hattingen E, et al. Myoinositol as a biomarker in recurrent glioblastoma treated with bevacizumab: a 1H-magnetic resonance spectroscopy study. *PLoS One*. 2016; 11(12):e0168113. <https://journals.plos.org/plosone/article?id=10.1371/journal.pone.0168113>
- Vaupel P, Schmidberger H, Mayer A. The Warburg effect: essential part of metabolic reprogramming and central contributor to cancer progression. *Int J Radiat Biol*. 2019; 95(7):912–919.
- De Feyter HM, Behar KL, Corbin ZA, et al. Deuterium metabolic imaging (DMI) for MRI-based 3D mapping of metabolism in vivo. *Sci Adv*. 2018; 4(8):eaat7314. https://www.science.org/doi/10.1126/sciadv.aat7314?url_ver=Z39.88-2003&rfr_id=ori:rid:crossref.org&rfr_dat=cr_pub%20%20pubmed
- Young RJ, Gupta A, Shah AD, et al. MRI perfusion in determining pseudoprogression in patients with glioblastoma. *Clin Imaging*. 2013; 37(1):41–49.
- Gahramanov S, Varallyay C, Tyson RM, et al. Diagnosis of pseudoprogression using MRI perfusion in patients with glioblastoma multiforme may predict improved survival. *CNS Oncol*. 2014; 3(6):389–400.
- Wan B, Wang S, Tu M, et al. The diagnostic performance of perfusion MRI for differentiating glioma recurrence from pseudoprogression: a meta-analysis. *Medicine (Baltim)*. 2017; 96(11):e6333. https://journals.lww.com/md-journal/Fulltext/2017/03170/The_diagnostic_performance_of_perfusion_MRI_for.40.aspx
- Talati P, El-Abtah M, Kim D, et al. MR spectroscopic imaging predicts early response to anti-angiogenic therapy in recurrent glioblastoma. *Neurooncol Adv*. 2021; 3(1):vdab060.
- Andronesi OC, Gagoski BA, Sorensen AG. Neurologic 3D MR spectroscopic imaging with low-power adiabatic pulses and fast spiral acquisition. *Radiology*. 2012; 262(2):647–661.
- Ogg RJ, Kingsley PB, Taylor JS. WET, a T1- and B1-insensitive water-suppression method for in vivo localized 1H NMR spectroscopy. *J Magn Reson B*. 1994; 104(1):1–10.
- Haase A, Frahm J, Hänicke W, Matthaei D. 1H NMR chemical shift selective (CHESS) imaging. *Phys Med Biol*. 1985; 30(4):341–344.
- Verma A, Kumar I, Verma N, Aggarwal P, Ojha R. Magnetic resonance spectroscopy—revisiting the biochemical and molecular milieu of brain tumors. *BBA Clin*. 2016; 5:170–178.
- Lange T, Dydak U, Roberts TPL, et al. Pitfalls in lactate measurements at 3T. *Am J Neuroradiol*. 2006; 27(4):895–901.

26. Ratai EM, Zhang Z, Snyder BS, et al. Magnetic resonance spectroscopy as an early indicator of response to anti-angiogenic therapy in patients with recurrent glioblastoma: RTOG 0625/ACRIN 6677. *Neuro Oncol.* 2013; 15(7):936–944.
27. Provencher SW. Automatic quantitation of localized in vivo ¹H spectra with LCModel. *NMR Biomed.* 2001; 14(4):260–264.
28. Howe FA, Barton SJ, Cudlip SA, et al. Metabolic profiles of human brain tumors using quantitative in vivo ¹H magnetic resonance spectroscopy. *Magn Reson Med.* 2003; 49(2):223–232.
29. Fedorov A, Beichel R, Kalpathy-Cramer J, et al. 3D Slicer as an image computing platform for the quantitative imaging network. *Magn Reson Imaging.* 2012; 30(9):1323–1341.
30. Batchelor TT, Gerstner ER, Emblem KE, et al. Improved tumor oxygenation and survival in glioblastoma patients who show increased blood perfusion after cediranib and chemoradiation. *Proc Natl Acad Sci USA.* 2013; 110(47):19059–19064.
31. Sidibe I, Tensaouti F, Roques M, Cohen-Jonathan-Moyal E, Laprie A. Pseudoprogression in glioblastoma: role of metabolic and functional MRI-systematic review. *Biomedicines.* 2022; 10(2):285. <https://www.mdpi.com/2227-9059/10/2/285>
32. Monteiro AR, Hill R, Pilkington GJ, Madureira PA. The role of hypoxia in glioblastoma invasion. *Cells.* 2017; 6(4):E45. <https://www.mdpi.com/2073-4409/6/4/45>
33. Zhang H, Ma L, Wang Q, et al. Role of magnetic resonance spectroscopy for the differentiation of recurrent glioma from radiation necrosis: a systematic review and meta-analysis. *Eur J Radiol.* 2014; 83(12):2181–2189.
34. Seeger A, Braun C, Skardelly M, et al. Comparison of three different MR perfusion techniques and MR spectroscopy for multiparametric assessment in distinguishing recurrent high-grade gliomas from stable disease. *Acad Radiol.* 2013; 20(12):1557–1565.
35. Rand SD, Prost R, Li SJ. Proton MR spectroscopy of the brain. *Neuroimaging Clin N Am.* 1999; 9(2):379–395.
36. Chuang MT, Liu YS, Tsai YS, Chen YC, Wang CK. Differentiating radiation-induced necrosis from recurrent brain tumor using MR perfusion and spectroscopy: a meta-analysis. *PLoS One.* 2016; 11(1):e0141438. <https://journals.plos.org/plosone/article?id=10.1371/journal.pone.0141438>
37. Duret V, Rossier C, Buck A, Stupp R, Prior JO. Performance of ¹⁸F-fluoro-ethyl-tyrosine (¹⁸F-FET) PET for the differential diagnosis of primary brain tumor: a systematic review and metaanalysis. *J Nucl Med.* 2012; 53(2):207–214.
38. Lapa C, Linsenmann T, Monoranu CM, et al. Comparison of the amino acid tracers ¹⁸F-FET and ¹⁸F-DOPA in high-grade glioma patients. *J Nucl Med.* 2014; 55(10):1611–1616.
39. Kratochwil C, Combs SE, Leotta K, et al. Intra-individual comparison of ¹⁸F-FET and ¹⁸F-DOPA in PET imaging of recurrent brain tumors. *Neuro Oncol.* 2014; 16(3):434–440.
40. Brahm CG, den Hollander MW, Enting RH, et al. Serial FLT PET imaging to discriminate between true progression and pseudoprogression in patients with newly diagnosed glioblastoma: a long-term follow-up study. *Eur J Nucl Med Mol Imaging.* 2018; 45(13):2404–2412.
41. Tiwari P, Prasanna P, Wolansky L, et al. Computer-extracted texture features to distinguish cerebral radionecrosis from recurrent brain tumors on multiparametric MRI: a feasibility study. *Am J Neuroradiol.* 2016; 37(12):2231–2236.
42. Jang BS, Park AJ, Jeon SH, et al. Machine learning model to predict pseudoprogression versus progression in glioblastoma using MRI: a multi-institutional study (KROG 18-07). *Cancers (Basel).* 2020; 12(9):E2706. <https://www.mdpi.com/2072-6694/12/9/2706>
43. Wen PY, Macdonald DR, Reardon DA, et al. Updated response assessment criteria for high-grade gliomas: response assessment in neuro-oncology working group. *J Clin Oncol.* 2010; 28(11):1963–1972.
44. Ma Y, Wang Q, Dong Q, Zhan L, Zhang J. How to differentiate pseudoprogression from true progression in cancer patients treated with immunotherapy. *Am J Cancer Res.* 2019; 9(8):1546–1553.
45. Melguizo-Gavilanes I, Bruner JM, Guha-Thakurta N, Hess KR, Puduvalli VK. Characterization of pseudoprogression in patients with glioblastoma: is histology the gold standard? *J Neurooncol.* 2015; 123(1):141–150.
46. Kim J, Chang KH, Na DG, et al. Comparison of 1.5T and 3T ¹H MR spectroscopy for human brain tumors. *Korean J Radiol.* 2006; 7(3):156–161.
47. Barker PB, Hearshen DO, Boska MD. Single-voxel proton MRS of the human brain at 1.5T and 3.0T. *Magn Reson Med.* 2001; 45(5):765–769.